Astron. Astrophys. 319, 98–108 (1997)

ASTRONOMY
AND
ASTROPHYSICS

The variation of abundances in planetary nebulae with height above the Galactic plane⋆

J. Köppen[1,2,4] **and F. Cuisinier**[1,3]

[1] Equipe 'Evolution Galactique', URA 1280, Observatoire de Strasbourg, 11 rue de l'Université, F-67000 Strasbourg, France
[2] Institut für Astronomie und Astrophysik der Universität, D-24098 Kiel, Germany
[3] Astronomisches Institut der Universität Basel, Venusstr. 7, CH-4102 Binningen, Switzerland
[4] International Space University, Parc d'Innovation, F-67400 Illkirch, France

Received 5 March 1996 / Accepted 24 July 1996

Abstract. In a sample of 94 planetary nebulae of the Galactic disk we find a systematic decrease of the abundances of He, N, O, S, and Ar with height above the Galactic plane, and also with radial velocity. Over an interval of 3 kpc the abundance of O, S, and Ar decrease by 0.1 ... 0.2 dex. This value is in good agreement with the predictions of an empirical model for the chemical and kinematical evolution of the disk, based on relations and constraints of the solar neighbourhood. The radial migration of the progenitor stars, caused by the velocity dispersion increasing with age, is found to be quite important for the vertical metallicity profile.

Key words: Galaxy: abundances – Galaxy: structure – Planetary nebulae: general – Galaxy: evolution

1. Introduction

The vertical structure of the Galactic disk is determined by how the various stellar populations settle into the gravitational potential. Gas and young stars have a low velocity dispersion (about 10 km/s in the vertical component) and thus are confined to a very thin disk with a scale-height of about 100 pc. Old stars have larger velocity dispersions and are found in heights up tp a few kpc. The shape of the relation between velocity dispersion and age of the stars allowed Wielen (1977) to deduce that this systematic increase is due to a continuous kinematical heating of the stellar population. While the origin of this process is probably gravitational encounters with other galactic objects, these collision partners have unfortunately not yet been identified.

Due to their conspicuous emission line spectra, planetary nebulae (PN) can be observed at large distances throughout the Galaxy, permitting to determine the chemical composition of the gas from which the progenitor star was born. The stellar life-times cover a wide range, roughly from 1 Gyr to 15 Gyr: The massive ($M_* > 3\,M_\odot$) short-lived stars produce nebulae enriched in helium and nitrogen, the products of stellar nucleosynthesis (Peimbert's (1978) Type I nebulae). Most nebulae however come from less massive stars ($M_* \approx M_\odot$) with long life-times which make PNs very useful as probes into the history of galactic evolution.

Thus, studies with PN allow to test the results of the stellar studies, limited to the solar neighbourhood, over a major portion of the Galactic disk. From a sample of about 60 nebulae, Kaler (1970) finds that the oxygen abundance is correlated with height above the plane and the difference of radial velocity and the value for a circular orbit, expected from the galactic rotation curve. Metal-rich planetaries are found only close to the galactic plane and at small velocity differences, while metal-poor objects can be found up to large heights and with large velocities. On the basis of these differences in spatial distribution and kinematics, he distinguishes two populations of PN, whose mean oxygen abundances differ by a factor 1.7, i.e. 0.2 dex. Barker (1978) determines the chemical compositions of 32 nebulae, and obtains a difference of only a factor 1.2 for the nebulae of the same two populations, less than the dispersion of the abundances. He concludes that the differences found by Kaler (1970) are 'either smaller or non-existant'. Though his observations and analyses are done in a homogeneous way, his sample is highly biased towards kinematically or chemically peculiar PN. With more recent observational material, Kaler (1980) finds a rather clear correlation between oxygen abundance, height above the plane, and radial velocity. There seems to be a distinct cut at 85 km/s above which no oxygen-rich nebulae are present. As his sample of 97 planetaries includes also halo objects, his findings may not strictly apply only to the disk. Faúndez–Abans & Maciel (1988) do not find any vertical gradient; only the four halo PN had lower abundances than the mean of the others.

In order to clarify this situation, Cuisinier et al. (1996) obtained high quality spectra of 62 planetary nebulae which were selected preferentially with large heights above the galactic

Send offprint requests to: J. Köppen (Kiel)

⋆ Partially based on observations collected at the European Southern Observatory, La Silla, Chile

plane and which give a good coverage in height. This sample turned out to be too small to yield definitive results. Therefore we combine this new data with high quality abundance analyses from other authors (Sect. 2). Using a common distance scale (Sect. 3) we investigate the relations between element abundances, height, and radial velocity in Sect. 4. A simple empirical model for the chemical and kinematical evolution of the solar neighbourhood is constructed (Sect. 5) which is compared to the PN data (Sect. 6).

2. Observational sample

To obtain a representative sample of planetary nebulae of the disk, we combine the data from the following studies: the surveys of Aller & Czyzak (1983) (41 objects) and Aller & Keyes (1987) (48 objects) constitute a fairly large and homogeneous set of high-quality observational material which gives reliable abundances. The analyses were done mainly by plasma diagnostics supplemented by the construction of individual photoionization models for the nebulae. More recent data is available on southern objects, from the survey by Kingsburgh & Barlow (1994) (65 objects) and our own data (Cuisinier et al. 1995) (62 objects, preferentially high above the Galactic plane). Both studies have similar signal-to-noise ratios and use plasma diagnostics. Thus the entire sample is composed of two sub-samples (AC+AK) and (KB+CAK) each of which can be regarded as quite homogeneous. For several objects in common, we use the more recent data, so that the complete sample contains 202 objects.

We do not make any distinction between abundances derived from plasma diagnostics or photoionization models, as both give very similar results, provided the quality of the observational material is sufficiently high, in particular if the weak diagnostic lines could be accurately measured (cf. Samland et al. 1992), which is the case for the objects in the sample. For our studies we use only the data accepted by the authors as reliable, i.e. those not marked with a colon. Furthermore, we concentrate only on nebulae with excitation class larger or equal to 4.5 (Aller's scale, Fig. 1 in Aller & Liller 1968). In these nebulae the abundance of helium is not marred by the unobservable neutral fraction, which can also affect the other elements' abundances via the ionization correction factors.

To investigate the vertical structure of the galactic disk, we should ideally study nebulae only in the solar neighbourhood, or at the same galactocentric distances as the sun. But in order to ensure a reasonable statistics, we must have a sample as large as possible. As a compromise, we pick out only nebulae that surely belong to the disk close to the sun. Our selection criteria are:

- use only nebulae whose the electron density (from the [S II] lines) has reliably been determined. This excludes objects whose line ratio is close to saturation. Thus, the distances can be derived from Barlow's method (see below), and the position in the Galaxy can be established.
- exclude halo planetary nebulae, such as PN G 108.4 − 76.1 (BoBn-1)

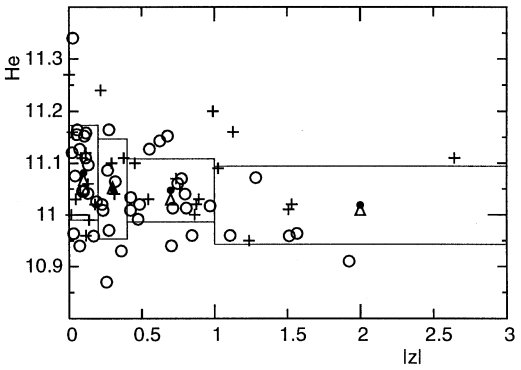

Fig. 1. The helium abundance of planetary nebulae as a function of their height $|z|$ (in kpc) above the Galactic plane. The crosses are abundance data from Aller & Czyzak (1983) and Aller & Keyes (1987), the open circles are from Kingsburgh & Barlow (1994) and Cuisinier et al. (1996), For the combined sample, mean abundances in each of 4 height bins are indicated by filled circles, and median values by the triangles; the vertical extension of each box shows the dispersion.

- reject nebulae that are likely to belong to the bulge (galactic longitude and latitude less than 10 degrees, and angular diametre less than 10 arcsec)
- exclude objects with distances larger than 15 kpc from the sun. This avoids a number of nebulae with small angular diametres whose available data appear suspect.
- take only nebulae whose linear distance from the axis of galactic rotation is between 3.5 and 15 kpc. This is a further restriction to the disk proper.

Applying these selections, the sample is reduced to 94 objects, 34 from the (AC+AK) subsample and 60 from the more recent data.

3. Distances

We compute statistical distances for each object in the same manner as Kingsburgh & Barlow (1992): If the nebula is optically thin to the Lyman continuum, i.e. density bounded, the assumption that all planetary nebulae have the same average ionized mass allows the estimation of its distance from the measured Hβ-flux $F(\mathrm{H}\beta)$ corrected for interstellar extinction c, and the angular diametre (Shklovskij 1955). If one assumes that the gas density n in the nebular shell is well represented by the electron density measured with the [S II] line ratio, one does not need to use the angular diametre which may be inaccurate or difficult to define. Barlow (1987) has calibrated this scale with Magellanic Cloud nebulae. Thus, the distance (in kpc) is given by:

$$d_{\mathrm{B}} = 1.11\ 10^{-6}\ M_{\mathrm{H}}^{0.5} n^{0.5} (F(\mathrm{H}\beta))^{-0.5} 10^{-0.5c} \qquad (1)$$

where we had set the electron temperature constant and equal to 10^4 K. The ionized hydrogen mass $M_{\mathrm{H}} = 0.217 \pm 0.079\,\mathrm{M}_\odot$ is taken from Barlow et al. (1992). The Hβ-flux is in erg cm^{-2} s^{-1}, and the density in cm^{-3}.

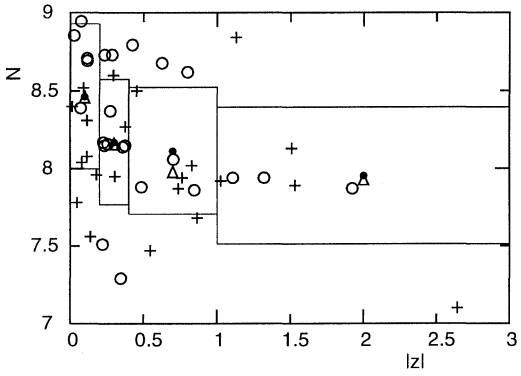

Fig. 2. Same as Fig. 1, but for nitrogen.

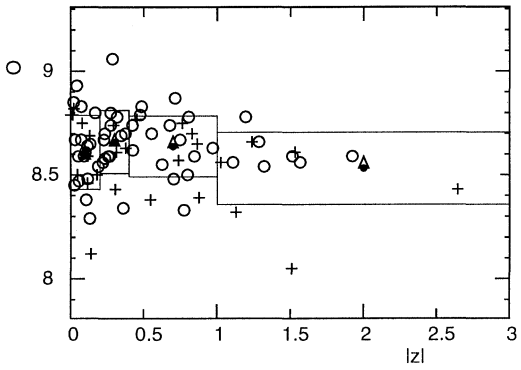

Fig. 3. Same as Fig. 1, but for oxygen.

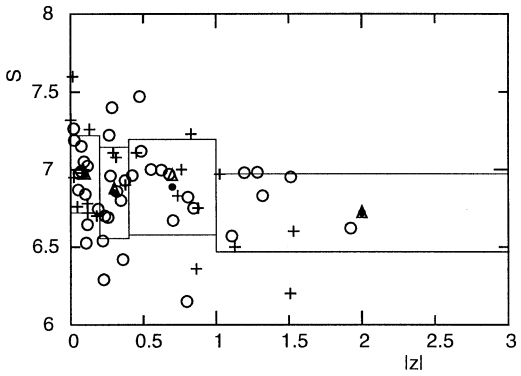

Fig. 4. Same as Fig. 1, but for sulphur.

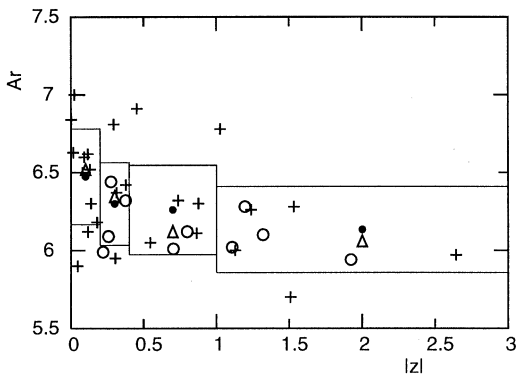

Fig. 5. Same as Fig. 1, but for argon.

In the early phases of evolution, the nebula is optically thick in the Lyman continuum and the central star evolves at constant luminosity. Then the assumption of a constant Hβ luminosity (Minkowski 1965) seems more appropriate:

$$d_{\rm M} = \left(\frac{L({\rm H}\beta)/4\pi}{F({\rm H}\beta)10^{c}}\right)^{0.5} = \left(\frac{F_1({\rm H}\beta)}{F({\rm H}\beta)10^{c}}\right)^{0.5} \quad (2)$$

Barlow et al. (1992) find from 28 optically thick PNs in the Magellanic Clouds an Hβ flux at a distance of 1 kpc $\lg(F_1({\rm H}\beta)) = -8.98 \pm 0.11$ [erg cm^{-2} s^{-1}].

When a nebula is optically thick, its ionized mass can expected to be smaller than the real mass; thus, the distance derived with the optically thin assumption overestimates the distance. Conversely, the Hβ luminosity of an optically thin nebula is smaller than if it were ionization bounded, and hence the Minkowski scale overestimates the true distance. Thus, the best estimate for the distance is

$$d = {\rm Min}(d_{\rm B}, d_{\rm M}) \quad (3)$$

The Hβ-fluxes are taken from the Strasbourg-ESO catalogue. The extinction measures c are taken from the individual analyses, with preference given to those values derived from the Balmer line decrement. The electron densities are also taken from the same studies, and whenever available and possible, the results of the [S II] lines are taken.

Of the 94 objects of the sample, 60 are optically thin and have Barlow distances (16 objects from AC+AK).

4. Observed patterns

4.1. Variation with height

The sample of nebulae is neither large enough nor complete in volume (nebulae close to the plane are under-represented) to permit the derivation of the density of objects in both metallicity and height above the Galactic plane. Therefore we show in Figs. 1 - 5 the dependence of the abundances of He, N, O, S, and Ar with height. In all the figures one notes a strong tendency of the maximum abundance of nebulae of the same height to decrease with height. There is no systematic difference between the data from the surveys by Aller and the more recent data. One may compute linear regressions through the data, and one finds a negative slope for all elements and in either sample. A more useful representation for the triangular shape of the plot is to compute the average abundances of the objects in various height groups. This is done in 4 groups with the bin borders placed at 0, 0.2, 0.4, 1, and 3 kpc to have roughly equal numbers of objects in each bin. While the number of nebulae is rather small and so the averages are somewhat sensitive to the placement of the bin limits, this type of plot gives a good indication of the trend that all abundances decrease with height above the plane. The

Table 1. The slopes of the decrease of the box-averaged abundances with height above the plane, and their errors. The values are given in dex/kpc, except for linear He and O abundances.

Elem.	slope from averages		slope from medians	
He	−0.027	±0.009	−0.028	±0.007
N	−0.21	±0.095	−0.22	±0.13
O	−0.055	±0.025	−0.041	±0.031
S	−0.11	±0.035	−0.12	±0.046
Ar	−0.15	±0.055	−0.21	±0.10
N/O	−0.12	±0.12	−0.18	±0.14
lin.He	−0.0076	±0.0026	−0.0069	±0.0020
lin.O	−0.066	±0.027	−0.047	±0.037

trend is present both in the averages and the median abundances. The slopes of linear regressions through either values, collected in Table 1, show significant negative values. The metallicity (O, S, Ar) thus decreases by about 0.15 to 0.3 dex over an 3 kpc interval. Nitrogen exhibits a steeper decrease, and a larger dispersion. The latter represents a large genuine variation of the nitrogen content among the nebulae (cf. Aller & Keyes (1987), Köppen et al. (1991), Samland et al. (1992)). In the plane, one finds a large number of nitrogen rich nebulae (cf. Sect.4.3).

The behaviour of the abundances with height is more pronounced, if one considers the linear abundances. In Fig. 6 we show for an example oxygen.

As the objects oscillate about the Galactic plane, their current height might be different from the maximal height which is the proper parameter describing the oscillation. We have tried to correct for this, by estimating the present vertical velocity component $v_z \approx v_{\rm rad} \sin b$ from the vertical projection of the measured radial velocity $v_{\rm rad}$, and computing the maximum height from $h_{\rm max} = \sqrt{h^2 + (v_z/\Omega)^2}$ where Ω = 40 km/s/kpc is the constant of the linear restoring force due to the gravitational potential, which we take from the Galactic model of Bienaymé et al. (1987). Since this correction is negligibly small (less than ten percent) for almost all nebulae, we shall not apply it at all.

The influence of the adopted distance scale is investigated by comparing with distances computed for all nebulae with a simple Shklovskij method, assuming an ionized mass of $M_{\rm H}$ = $0.2\,{\rm M}_\odot$ and a volume filling factor ϵ = 0.75, and using the optical angular diametres from the Strasbourg-ESO catalogue. Fig. 7 shows that while the heights above the plane tend to be smaller, the basic structure of the diagram does not change: both maximum and average abundances decrease with height above the plane.

4.2. Variation with radial velocity

The abundance-height relations are sensitive to the distances, and thus may be affected by corresponding uncertainties. An independent check is to look at the relation between abundances and radial velocity. In Fig. 8 we show the relation for the (linear) oxygen abundance. One notes another clear trend: the maximum abundance decreases with increasing velocity. This fully confirms the findings of Kaler. But in comparison with Kaler's (1980) Fig. 1, we emphasize that in our sample there are no objects of radial velocity greater than 200 km/s. This is because of our selection of objects of the nearby disk, and in particular of the exclusion of halo and bulge nebulae. The "sudden drop" of the oxygen abundance at 85 km/s noted by Kaler (1980) is not confirmed. Instead, we find a rather smooth variation of the maximum oxygen abundance. In view of the small number of nebulae at large velocities, and the finite accuracy of the abundance determinations (±0.1 dex for oxygen, e.g. Cuisinier et al. 1996) it could well be that the drop was but a spurious feature in Kaler's sample.

Kaler (1970) distingushes two populations: PN of the presumably younger one are close to the disk (within 0.8 kpc) and their radial velocity differs by less than 60 km/s from the value predicted for a circular orbit from the Galactic rotation curve. The average oxygen abundance of these nebulae is found to be about 0.2 dex higher than that of the other population which is formed by PN with either great heights or large velocities. Applying the same criteria to our sample, we find for the first group from 39 nebulae a mean oxygen abundance of 8.65 ± 0.03 with a dispersion of 0.16 ± 0.02, while the second group (of 41 PN) yields an average of 8.58 ± 0.03 and a dispersion of 0.17 ± 0.02.

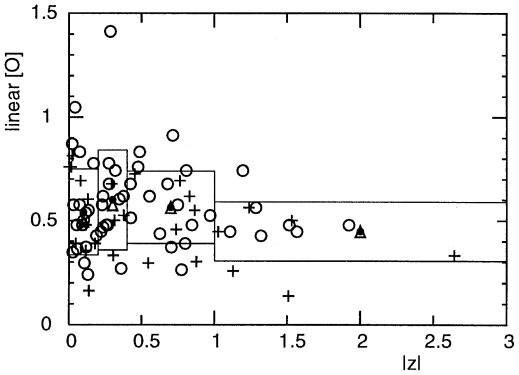

Fig. 6. Same as Fig. 3, but for the linear oxygen abundance (solar value = 1.0).

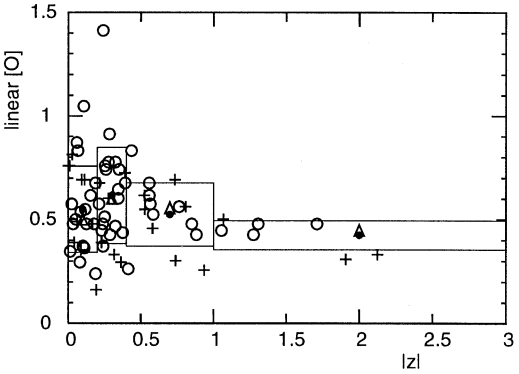

Fig. 7. Same as Fig. 6, but using Shklovskij distances for all objects.

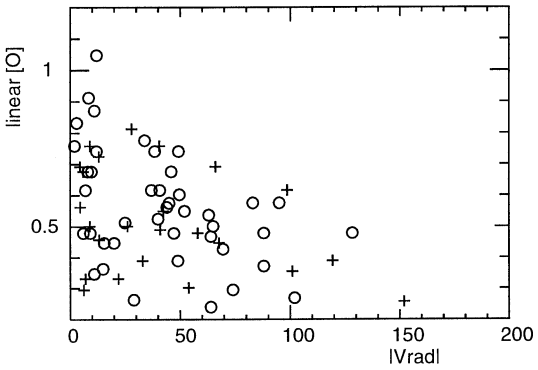

Fig. 8. The (linear) oxygen abundance (solar = 1.0) of planetary nebulae as a function of their radial velocity. Same symbols as in Fig. 1.

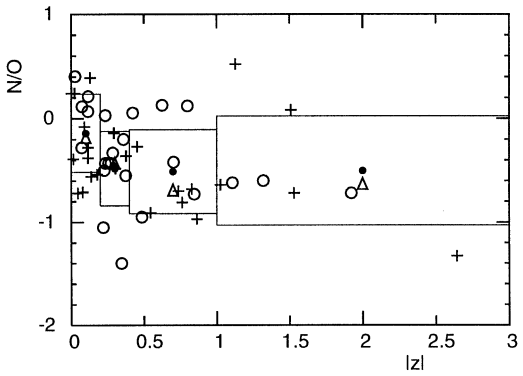

Fig. 9. Same as Fig. 1, but for the abundance ratio N/O.

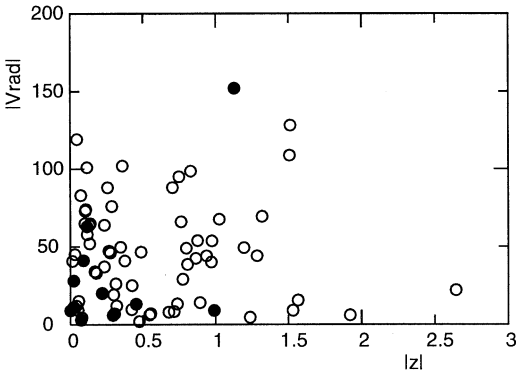

Fig. 10. The heights above the plane and the radial velocity of type I planetary nebulae (filled circles) and non-type I objects.

Thus, the averages differ significantly, but by only about 0.1 dex, which is quite comparable to what Barker (1978) obtained.

4.3. Type I nebulae

The abundance ratio N/O also exhibits a clear decrease with height (Fig. 9), despite the large scatter. Since helium and nitrogen are enriched in planetary nebulae with more massive progenitors, in which these elements had been synthesized, this indicates that the younger nebulae are preferentially found close to the Galactic plane. Among the 94 nebulae used of the whole sample, there are 11 objects that are of Peimbert's (1978) type I, being rich in both helium (He $>$ 11.10) and nitrogen (N/O > -0.3). In Fig. 10 we compare the heights above the plane and the radial velocities for type I and all other nebulae. The strong concentration of the type I objects to the galactic plane and to small radial velocities as well clearly shows that these PN are younger than the non-type I objects, as one would expect. Because of this small number of objects, and because our sample is not statistically complete, we refrain from comparing these data with predictions for type I nebulae from our model which is described in the next section. Only two nebulae are high above the plane, at about 1.2 kpc: PN G 100.0 − 08.7 (Me 2 − 2) has a large radial velocity (-152.0 km/s) and might not be a disk object, and 006.3 + 04.4 (H 2 − 18).

5. Chemical evolution model

In order to compare our findings on the decrease in metallicity of PNs with height above the plane with what is known about the vertical structure of the disk from stars, we construct a simple empirical model of the chemical and kinematical evolution of the solar neighbourhood. In doing so, we make use of observed properties as much as possible, and avoid making assumptions about the processes of in the disk (gas infall, dependence of the star formation rate (SFR) on the gas density etc.) and questions of uniqueness of the particular model.

We treat the vertical structure of the solar neighbourhood in the following one-dimensional model: All star formation takes place in the plane of the disk. With time, the stars acquire a dispersion of the vertical velocity component W, and each age group is distributed as an isothermal component in the gravitational field. This field is assumed to be constant in time, and to be caused by the presently observed gas and stars. Likewise, the stars acquire an increase of the dispersion of the U-velocity, and thus stars born outside the solar vicinity may be found in the local neighbourhood at the present time.

For the description of the disk PN population it is sufficient to know the history of star formation, chemical enrichment, and kinematic properties, irrespective of how these came about physically, and when and how the disk was formed. We chose simple analytical formulations which agree with observational constraints in the solar neighbourhood:

5.1. Age-metallicity relation

The age-metallicity relation of the solar neighbourhood stars has been derived by Meusinger et al. (1991). They made a simple model which yields a convenient function of time $t = T - a$ in Gyrs:

$$[\mathrm{Fe/H}](t) = \log(1.98 - 1.88(1 - t/28.5)^{1.25}) \qquad (4)$$

with an age of the disk T = 15 Gyrs. This is almost identical to the linear iron abundance increasing linearly with time from an

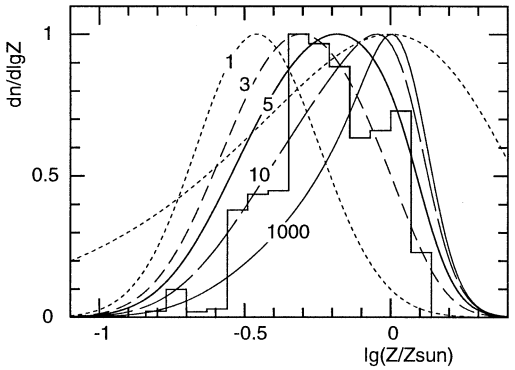

Fig. 11. The metallicity distribution function of the G dwarfs, as observed (histogram, from Pagel 1989), and as computed from our simple model. The dashed lines shows results obtained with a SFR decreasing exponentially with the indicated time constant (in Gyrs), the thick full line is the 'standard' model with $\tau_{\rm SFR}$ = 5 Gyr, the broad dashed curve is the Simple Model. To account for uncertainties in the abundance determinations, the model distributions are convolved with a gaussian of an abundance dispersion of 0.075 dex.

initial value of 0.1 to a present value of 1.16 of the solar value. Conversion to oxygen abundance is done using the recommendation of Pagel (1992):

$$[\mathrm{O/H}] = 0.7 \cdot [\mathrm{Fe/H}] \quad \text{for} \quad [\mathrm{Fe/H}] > -1.0 \tag{5}$$

5.2. Star-formation rate

If we took this AMR and a SFR constant in time, the metallicity distribution of the G dwarfs comes out narrower than observed (from Pagel 1989), while the closed box 'Simple Model' gives too broad a distribution (Fig. 11). A good match of the empirical function is provided by a SFR which decreases moderately in time:

$$\Psi(t)/\Psi(0) = \exp(-t/5\,\mathrm{Gyr}) \tag{6}$$

We chose an exponential function because only one free parameter needs to be determined. In Fig. 11 we show the metallicity distribution function of the G-dwarfs (main-sequence mass below 0.8 $M_\odot$). Certainly, the fit with 5 Gyrs (which we shall call the 'standard' model) is not perfect, but we find that any amount of additional sophistication (cf. Meusinger 1994) does not affect the conclusions on planetary nebulae. We note that more elaborate chemical evolution models that are successful in explaining both the AMR and the G-dwarf distribution (e.g. Matteucci & François 1989, Köppen & Arimoto 1990, Sommer-Larsen & Antonuccio-Delogu 1993) imply that the time scales for gas infall and star formation should be similar, which results in a SFR varying moderately with time.

At each age $a = 0...T$ up to the age T = 15 Gyr of the Galaxy, we compute the contribution to the surface density N of presently visible planetary nebulae by formation of progenitor stars with ages between a and $a + \Delta a$:

$$N(a)|\Delta a| = \Psi(T-a)|\Delta a| \cdot \int_{m_1}^{m_2} \phi(m) dm \tag{7}$$

Since we shall be dealing with relative distributions, the absolute value of the SFR – $\Psi(0)$ – is of no importance here. The integration over stellar initial masses is done only over those which produce presently observable PN:

$$m_1 = \max(m_{\rm low}, m(T - a - \tau_{\rm PN}))$$

and

$$m_2 = \min(m_{\rm high}, m(T - a))$$

using a simple relation between stellar lifetime and main-sequence mass:

$$\tau_m = 0.03 + \frac{10}{m^2}$$

in Gyrs and $M_\odot$. The mass range for the progenitor stars is taken as 0.8...5$M_\odot$. The life-time of a PN, i.e. during which it can be observed, depends on the time-scales for stellar and nebula evolution. For simplicity, we took a constant life-time of $\tau_{\rm PN}$ = 30 000 yrs. This tends to overestimate the steepness of the vertical metallicity profile: Since more massive progenitors probably give more massive central stars which evolve more rapidly, their PN are less likely to be observed. This reduces the effective range of progenitor masses and the age range for the present PN. A variation of the life-time by a factor 100 would reduce the abundance difference from 0.20 dex to 0.13 dex. The initial mass function ($\phi(m)dm$ specifies the number of stars in the interval $m...m + dm$) is a power law $\phi(m) \propto m^{-2.35}$ (Salpeter's IMF) in the mass range from 0.05 to 60 $M_\odot$.

5.3. Age-velocity-dispersion relation

The PN progenitor stars are assumed to have a dispersion of the vertical velocity component W which increases with the age of the stars. The observed age-velocity-dispersion relation (AVR) is well described by Wielen (1977):

$$\sigma_v = \sqrt{100 + 600a} \tag{8}$$

in km/s, with a in Gyrs. This also matches very well the data from the stars in the solar vicinity (Jahreiß & Wielen 1983). We assume a constant velocity ellipsoid with

$$\sigma_{\rm U} : \sigma_{\rm V} : \sigma_{\rm W} = 0.79 : 0.46 : 0.41$$

as observed, as compared to the prediction of diffusion theory of 0.77 : 0.49 : 0.41 (Wielen 1977). With these relations one obtains $\sigma_{\rm W}$ for each age group. All stars in a group are assumed to form an isothermal population which has settled into the gravitational potential $\Phi(h)$, and the space density n of nebulae as a function of height h above the Galactic plane is computed as

$$n(h,a) = n_0(a) \exp(-\frac{\Phi(h)}{\sigma_{\rm W}^2}) \tag{9}$$

The space density in the plane $n_0(a)$ is determined from the normalization

$$2\int_0^\infty n(h,a)dh = N(a) \tag{10}$$

The gravitational potential Φ is assumed to be constant in time, and is calculated by integrating over the galactic mass distribution as described by the sum over all components (stars and gas) of the Besançon model (Bienaymé et al. 1987).

Since Φ does not change as the vertical distribution of stars changes, there is no difference between the velocity dispersion increasing with stellar age or decreasing as the disk evolves. Therefore, we cannot and do not distinguish between these two complementary interpretations of the AVR.

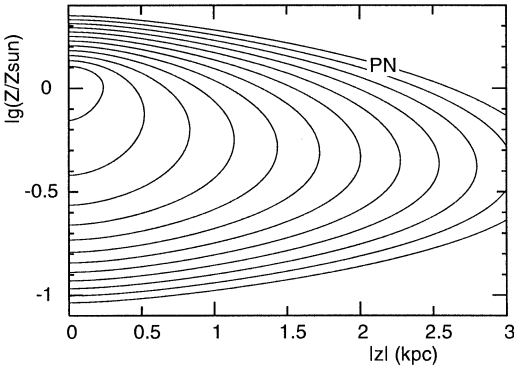

Fig. 12. The density of planetary nebulae per unit height and metallicity interval. The contour lines are spaced by 0.25 dex.

5.4. Radial diffusion of progenitor stars

If the progenitor stars remained always at the same galactocentric distance where they were born, the AMR (Eq. 4) determines the metallicity Z_0 of this age group, which is used to find the (logarithmic) metallicity bin to which the corresponding contribution is to be added:

$$n(h, \lg Z_0)|\Delta \lg Z| = n(h,a)\Delta a \tag{11}$$

Instead, due to the velocity dispersion in radial direction – which also increases with age – stars that were born at different galactic radii can enter the solar neighbourhood where they may produce a planetary nebula. Due to the radial abundance gradient in the disk, the metallicity of these nebulae differs accordingly.

To take into account the contribution to local nebulae by the stars that were born at age a at galactocentric radius r, we assume that the SFR, AMR, and AVR do not change with radius, so that we may use the densities computed for each age group also for other radii. The radial abundance gradient in the disk is assumed to be constant in time, which is supported by the measurement of abundance gradients with planetary nebulae of different age groups (Maciel & Köppen 1994). For oxygen we use $d\lg Z/dr = -0.07$ dex/kpc. For any age group with a metallicity Z_0, nebulae with a different metallicity Z originate from galactocentric radius r

$$r - \mathrm{R}_\odot = \frac{\lg Z/Z_0}{d\lg Z/dr} \tag{12}$$

The distribution function of stars which have diffused over this radial distance $\mathrm{R}_\odot - r$ can well be represented by a gaussian function centered at the galactocentric radius r at the time of birth, with a dispersion $\sigma_\mathrm{R}(a)$. This dispersion is determined by the growing amplitudes of the radial excursions of the stellar orbits $\sigma_\mathrm{U}(a)/\kappa$. In the model of the constant isotropic diffusion coefficient for the stellar orbits (Wielen 1977) there is an additional contribution by the changes of the galactocentric distance R_m of the guiding centres for the stellar epicycles. This amounts to

$$\sigma^2_{R_m} = \frac{D\tau}{(2B)^2} = \frac{2\sigma^2_\mathrm{U}}{\kappa^2 + (2B)^2} \tag{13}$$

$$= 2.44\left(\frac{\sigma_\mathrm{U}}{\kappa}\right)^2 \tag{14}$$

(cf. Wielen et al. 1996). The epicyclic frequency κ = 31.6 km/s/kpc is obtained with conventional values for Oort's constants (A = 15 km/s/kpc, $B = -10$ km/s/kpc at $\mathrm{R}_\odot$ = 8.5 kpc). Both effects combined give $\sigma_\mathrm{R}(a) = 1.56 \cdot \sigma_\mathrm{U}(a)/\kappa$ (Fuchs et al. 1994, 1995).

Because the density in the stellar disk increases inward, the contribution from stars closer to the galactic centre is larger. We assume an exponential function with a (constant) radial scale-length of r_ℓ = 4 kpc (cf. Bienaymé et al. 1987).

Altogether, the contribution of nebulae of a given age group to height bins h and metallicity bins lg Z is given by:

$$n(h,\lg Z)|\Delta\lg Z| = n(h,a)\cdot|\Delta a|\cdot\exp(-\frac{r-\mathrm{R}_\odot}{r_\ell})\cdot \frac{1}{\sqrt{2\pi}\sigma_\mathrm{R}}\exp(-\frac{(r-\mathrm{R}_\odot)^2}{2\sigma^2_\mathrm{R}}) \tag{15}$$

where r follows from Eq. 12.

At all time steps, these contributions $n(h, \lg Z)$ are added to the appropriate bins, and one obtains the overall distribution function of planetary nebulae in height und metallicity. In order to get well defined, smooth distribution functions, 10000 time steps suffice.

5.5. Sensitivity of the parameters

Since all functions that go into the model are subject to uncertainties, we investigated how the results are changed, if other parametrizations are utilized.

A longer timescale for the decline of the star formation rate increases the fraction of younger nebulae, which are metal-rich and closer to the plane. This leads to a steeper drop of abundance with height. Using in the 'standard' model τ_SFR = 1, 3, 5, 10, 1000 Gyr one gets for the difference of the mean abundance between the first and last bin: 0.03, 0.14, 0.20, 0.25, 0.29 dex. Fig. 11 shows that τ_SFR = 3...10 would be the maximum range of models compatible with the G dwarf distribution.

The data of Edvardsson et al. (1993) can be well represented by a linear relationship between age and logarithmic iron abun-

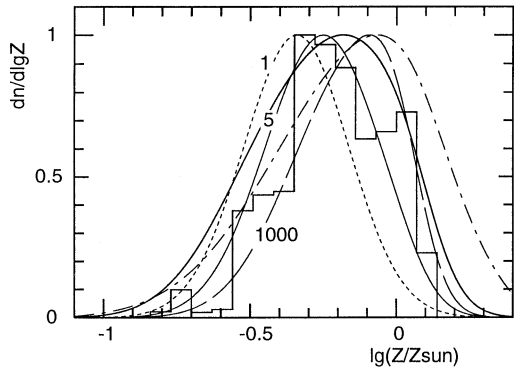

Fig. 13. Same as Fig. 11, but computed with the AMR fitted to the data of Edvardsson et al. 1993. The dashed curves are three models with different decline times of the star formation rate, in comparison with the 'standard' model (thick full line). The dash-dotted line shows how the results change if one increases in the standard model the radial dispersion σ_R by a factor of 1.56 to account for diffusion of the guiding centres of the stellar orbits.

dance (Wielen et al. 1996):

$$[\mathrm{Fe/H}] = 0.05 - 0.048 \cdot (a/\mathrm{Gyrs})$$

If this function ist used, the metallicity distribution function of the G dwarfs (Fig. 13) is somewhat narrower than the one computed with the AMR of Meusinger et al. (1991), but which would be equally acceptable. The influence by the star formation time scale is quite weaker, thus values different from 5 Gyrs would be acceptable. For the observable decrease of the mean PN metallicity with height above the plane one finds a flatter slope (cf. Fig. 15): The abundance decrease between 0 and 3 kpc height is changed from 0.20 dex ('standard' model) to only 0.11 dex.

Meusinger et al. (1991) derived a different shape of the velocity ellipsoid than Wielen:

$$\sigma_U : \sigma_V : \sigma_W = 0.68 : 0.50 : 0.54$$

The overal effect on the PN metallicity profile is negligible, as the larger ratio σ_W/σ_v yields a flatter distribution in heights, which is compensated by the smaller ratio σ_U/σ_v resulting in a smaller influence of the radial diffusion: the abundance difference is 0.23 dex.

The exact shape of the AVR has not a very strong effect on the PN metallicity profile. If one uses as a fit to the measured velocity dispersions (Fuchs et al. 1995) instead of the square-root function a simple straight line

$$\sigma_v(a) = 20 + 5.8 \cdot (a/\mathrm{Gyr}) \quad \mathrm{km/s} \tag{16}$$

one gets almost the same metallicity profile (see Fig. 14) with a drop in abundance of 0.22 dex. If the AVR was a straight line, connecting the values of Wielen's AVR at ages 0 and 15 Gyr – which is already a poor representation of the data – the PN metallicity profile changes only insignificantly: the abundance drop is 0.24.

Using a smaller radial scalelength of the disk density profile (2.5 kpc), or increasing the radial abundance gradient (-0.1 dex/kpc) result in a stronger influence by the radial migration of the stars, and lower the vertical difference of the abundance from 0.20 dex to 0.18 dex and 0.19 dex, respectively.

Thus the most important parameters are the SFR and the AMR, which describe the chemical evolution. The empirical determination of the AMR is marred by the large scatter in the stellar data (cf. Meusinger et al. 1991) and by the large amount of what seems to be intrinsic scatter (Edvardsson et al. 1993). In our simple model, the SFR is adjusted to give a good fit to the G dwarf metallicity distribution. Fig. 13 shows that the inclusion of the radial diffusion of the guiding centres can change this distribution quite strongly: The peak is shifted by more than 0.1 dex towards higher metallicities because of metal-rich stars scattered from the region inside the solar circle. This shows that the pollution of the solar vicinity can be rather strong, and this should be taken into account when deriving the AMR. It may be desirable to do a more consistent modeling of the solar neighbourhood, with proper attention of the scatter in the stellar data, but this is somewhat outside the scope of this paper.

6. Comparison with observations

In the model, the mean abundance decreases systematically with height above the plane, as is illustrated by Fig. 14. The influence of radial wandering of the progenitor stars is quite important: without it, the abundance drops by 0.23 dex over an interval of 3 kpc. If only the radial excursions of the epicycles are taken into account ('standard' model), one gets 0.20 dex, but if the radial diffusion of the guiding centres are also included, the difference lowered to 0.16 dex. Likewise, the metallicities increase in general, because of the larger proportion of metal-rich progenitor stars that were born inside the solar circle. Comparison with the empirical data (note that Fig. 14 has the same logarithmic range for the oxygen abundance as Fig. 3), shows that the observed abundance variations of 0.1 ... 0.2 dex are well matched by models that include the radial wandering of the progenitor stars. The limitations of the observational data do not permit to reliably discriminate whether the radial diffusion of the guiding centres needs to be included. But the predictions on the basis of Wielen's (1977) constant and isotropic diffusion match the empirical data well.

The theoretical dispersion of the abundances is 0.20 ... 0.22 dex. Radial diffusion of the stars increases this value to 0.25 dex. Again, this is in good agreement with the observed values of about 0.2 dex, being somewhat less for O, and larger for S and Ar.

For this comparison, one also needs to consider the influence of the errors in the observational data, namely in the abundances and the nebular distances, and the averaging over galactocentric radii:

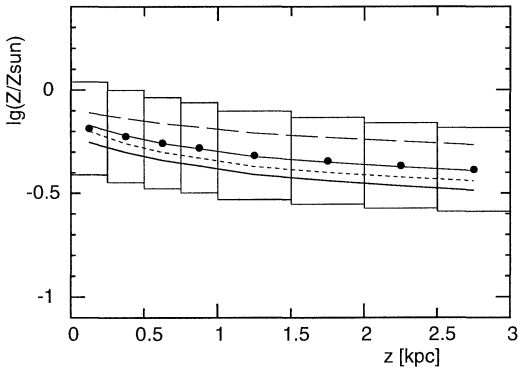

Fig. 14. The computed vertical dependence of the metallicity in planetary nebulae, in the 'standard' model. As in Fig. 1ff, the boxes indicate height bins, whose average metallicity is marked as the filled dot in the bin centre, and whose dispersion is shown as the vertical extension of each box. Note that the same range of coordinates as in Fig. 3 is depicted. The run of the averages from other models are shown as lines: neglect of radial wandering of stars (thick full line), inclusion of radial diffusion of guiding centres (long dashes), linear fit to AVR (thin line), linear AVR (short dashes).

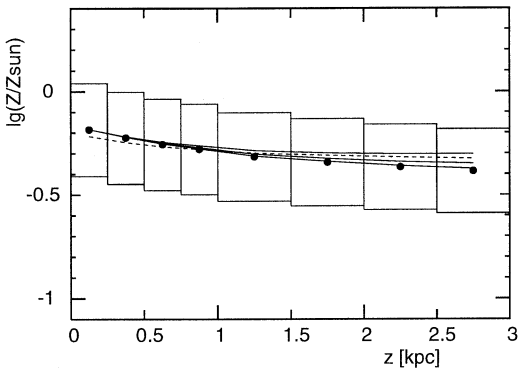

Fig. 15. Same as Fig. 14, but showing the influence of a relative error of σ_z/z = 0.1, 0.2, and 0.3 in the distances (full lines). The dashed line refers to a model with an AMR matched to the Edvardsson et al. (1993) data.

6.1. Errors in the abundances

Estimates on the errors of the abundances can be found in the individual analyses. Cuisinier et al. (1996) gave an account of the errors There are 8 objects that were also analyzed by Kingsburgh & Barlow (1994). Comparing the abundances, Cuisinier et al. have helium higher by 0.012 dex (with a dispersion of 0.046 dex), and oxygen abundances lower by 0.032 dex (dispersion 0.16 dex). Thus there is no significant systematic difference, but the dispersions give an indication of what the total errors might be.

From the model, one would expect a dispersion in the oxygen abundance of 0.2 dex. If one assumes that the abundance error is 0.16 dex, one gets 0.26 dex, which still is in agreement with the observations.

6.2. Distance errors

The errors of the distances are estimated from the errors of the utilized observational quantities, assuming gaussian distributions for the errors in all variables. The total relative error in the distance derived with Barlow's method is:

$$(\sigma_{dB}/d)^2 = (0.5\,\sigma_M/M)^2 + (0.5\,\sigma_n/n)^2 \quad (17)$$

$$+(0.5\,\sigma_F/F)^2 + (0.5\,\sigma_c)^2 \quad (18)$$

since e.g. the contribution to σ_d due to the uncertainty in the ionized mass M can be estimated as $0.5 d\sigma_M/M$ (from Eq. 1). Likewise, one gets for the Minkowski distances:

$$(\sigma_{dM}/d)^2 = (0.5\,\sigma_L/L)^2 + (0.5\,\sigma_F/F)^2 + (0.5\,\sigma_c)^2 \quad (19)$$

Let us estimate the errors of the various quantities: Comparing the electron densities derived by Cuisinier et al. (1996) with those determined by Kingsburgh & Barlow (1992, 1994) and Kingsburgh & English (1993) for the 8 objects in common, we get a dispersion of 0.1 dex, i.e. σ_n/n = 0.23. For the error in the absolute fluxes we adopt 0.1 dex as an upper limit to the errors given in the Strasbourg-ESO catalogue. Tylenda et al. (1992) compare the extinctions derived from the spectra of the ESO-Strasbourg survey (Acker et al. 1992) with those from other studies, and find a scatter between the values obtained from the Balmer lines to be $\sigma(\Delta c)$ = 0.2. Since for large values of c, the values derived from the ratio of Hβ- and radio-flux tend to be smaller by 0.16 than those determined from the Balmer lines, we adopt σ_c = 0.3. The error in the Hβ luminosity we take as 0.1 dex from Barlow et al. (1992) and inspection of the Strasbourg-ESO catalogue. For several objects it is substantially better. If one neglects an intrinsic spread of the ionized mass – but see the discussion at the end of this section – we get for both cases the same relative error in the distance of σ_d/d = 0.2.

Eqs. 17 and 19 show that the total distance error is equally sensitive to all individual uncertainties, and no single observational parameters is therefore particularily critical. But, since an absolute error of σ_c = 0.23 in the extinction is equivalent to a 0.1 dex relative error in the flux, the accuracy of c is quite a limitation, especially for highly reddened nebulae. Tylenda et al. (1991) pointed out that the extinctions derived from the Balmer decrement are systematically larger than those obtained with the ratio of the Hβ-flux to the radio continuum flux. Hence, if we used c from the Hβ-radio method, we should get smaller distances and a steeper vertical abundance profile, quite similar to the effect by using Shklovskij distances (cf. Figs. 6 and 7). Because the origin of the discrepancy in the c-values is still not fully understood, none of the two methods can really be preferred. Since in the determination of the Balmer decrement one measures the line fluxes with the same instrument, and one usually relies on several Balmer lines, we decided to prefer these values. In any case, the range over which the abundances vary is not affected.

In Fig. 15 we show the standard model, simulating the effects of a constant relative error σ_h/h in the height. This is done by convolving the distribution function $n(h, \lg Z)$ at each

metallicity bin by a gaussian function in height with the appropriate width σ_h. Evidently, the errors in the distances introduce a further smoothing on the vertical metallicity profile: the abundance difference over 3 kpc is reduced from 0.20 dex to 0.19, 0.17, and 0.12 dex for errors of 10, 20, and 30 percent.

From studies of nebulae with distances determined by independent methods, the ionized mass is known to exhibit quite a large range of values (e.g. Pottasch 1996). This applies not only to optically thick nebulae which may contain a large neutral fraction, but also to optically thin, evolved nebulae, such as K 1-27 which has a very small mass (Rauch et al. 1994). Because of the selection effects involved, we do not try to simulate this in our model. But we note from Fig. 15 that the model would be in agreement with the oxygen abundance profile, if the distance error were about 30 percent. If it were entirely due to the mass spread, one gets about 0.25 dex for the dispersion in the ionized mass of the nebulae in our sample.

6.3. Averaging over the Galactic disk

We included planetary nebulae from all galactocentric radii in order to have a sufficiently large sample of objects. Since there is a radial abundance gradient in the disk, the integration over a range in galactocentric distances results in a further averaging of the abundances of each height group. Nothing is known whether the radial gradient changes with height above the plane. We assume for simplicity that the radial metallicity gradient is constant for all heights and times: $d\lg Z/dr = -0.07$ dex/kpc. In each height bin, the PN distribution function is folded with a box-car function of width ± 0.35 dex, corresponding to a range of ± 5 kpc in galactocentric radius. Because we assumed a logarithmic abundance gradient – as is supported by the observations in our Galaxy and other spiral galaxies – the average (logarithmic) metallicities for each height above the plane are not changed by this convolution. Thus, the use of a sample of PN from all parts of the disk would not seriously affect the size if the decrease of mean abundances with height.

6.4. Discussion

Comparing with the effect of the radial diffusion of the progenitor stars, we note that a 20 percent distance error has the same influence on the vertical abundance profile as an increase of $\sigma_{\rm R}$ by a factor of 1.56 due to application of the diffusion theory for the velocity dispersions. The only difference is that in the latter case the mean metallicities are also increased due to the migration of more metal-rich stars into the solar vicinity. Since that would be nearly impossible to detect, one cannot separate the effects of radial diffusion from those due to distance errors.

If one wanted to explain an abundance difference of only 0.1 dex, this could be done by assuming either a larger distance error of 30 percent – which would not be in violent disagreement with our estimate – or that the value for $\sigma_{\rm R}$ is larger by a factor of 1.56, or any suitable combination thereof. The value of $\sigma_{\rm R}$ is determined by the age velocity-dispersion relation and the ratio for the dispersions of the velocity components, all of which are subject to an appreciable amount of uncertainty. The values we adopted here are averages over the rather small number of values from the Table 1 of Wielen (1977), which shows by itself a fairly large scatter.

7. Conclusions

From a sample of planetary nebulae with high-quality spectra we defined a group of 94 nebulae that belong to the galactic disk, and may therefore represent the solar neighbourhood. Among these objects, we find a systematic decrease of the abundances – as averaged over height intervals – of He, N, O, S, and Ar with height above the plane. For oxygen, sulphur, and argon this amounts to about 0.1...0.2 dex between $z = 0$ and $z = 3$ kpc. The abundances also show a systematic decrease with the radial velocity of the objects. Type I nebulae are found in low heights above the disk and with low radial velocities. These results confirm the earlier findings by Kaler (1970) and (1980).

A simple empirical model for the chemical and kinematic evolution of the solar neighbourhood is constructed, using the empirical age-metallicity-relation, the G-dwarf metal distribution function, and the age-velocity-dispersion relation. The progenitor stars are assumed to be born in the plane, and reach greater heights due to the velocity-dispersion that increases with age. Also, we take into account that the stars diffuse in radial direction, and we simulate the influence from the uncertainties of the nebula distances. This model predicts an abundance change of 0.1...0.2 dex, in good accord with the observational findings.

Separating the PN into two populations, using the Kaler's (1970) criteria on height above the plane and radial velocity, we find that nebulae close to the plane and on circular orbits have an average oxygen abundance larger by about 0.1 dex than the other nebulae. This is less that what Kaler (1970) gets, but agrees with Barker's (1978) result. Since a difference of that size is also well in agreement with the predictions of our model, we conclude that Barker already obtained quite a reasonable value, but drew too pessimistic a conclusion. The observational data and the model interpretation thus fully confirms the basic findings of Kaler (1970, 1980), but also shows that Barker's (1978) results are not in disagreement.

The agreement between model and observations is well within the uncertainties for the assumptions of the chemical and kinetic evolution (SFR, AMR, and AVR). Thus we may conclude that the 'classical' model of the evolution of the stellar disk by some form of dynamical heating of the stars in conjunction with our empirical understanding of the chemical evolution in the solar neighbourhood is consistent with the data obtained from planetary nebulae on the vertical metallicity structure of the disk.

Can one go further, adding more evidence in favour of or against diffusion theory for the stellar orbits, or discerning any indications for the initial settling of the gas into the present disk? In our empirical model the structure of the disk (radial density and metallicity gradient, gravitational potential) remains fixed. Thus one cannot distinguish in the AVR whether σ_v increases with stellar age or decreases with disk evolution. But as the ver-

tical metallicity profile is found not to be very sensitive to the exact shape of the AVR, it seems unlikely that the metallicity decrease could provide an identification of the physical origin of the AVR. On the other hand, one noticed that the amount of radial migration of the stars has a rather important influence. This could give a possible test for the diffusion theory, due its value of σ_R/σ_U containing the additional diffusion of the guiding centres. Such a test would still be rather hard, since it requires not only a larger sample and more accurate PN distances, but also that the chemical evolution (SFR and AMR) could be fixed more precisely.

Acknowledgements. We thank B. Fuchs, A.Just, G. Stasiǹska, R.Wielen, and A.Zijlstra for helpful discussions. Financial support is gratefully acknowledged by J.K. from the Deutsche Forschungsgemeinschaft (project He 1487/13-1), the CNRS, and the Université Louis Pasteur, Strasbourg.

References

Acker A., Ochsenbein F., Stenholm B. et al., 1992, "The Strasbourg–ESO catalogue of galactic planetary nebulae", ESO publ.
Aller L.H., 1987, in 'Spectroscopy of Astrophysical Plasmas', ed. A.Dalgarno, D.Layzer, Cambridge Univ.Press, Cambridge, p. 89
Aller L.H., Liller W., 1968, in *Nebulae and Interstellar Matter*, eds. B.M.Middlehurst, L.H.Aller, Univ.Chicago Press, Chicago, p.483
Aller L.H., Czyzak S.J., 1983, ApJ Suppl.Ser. **51**, 211
Aller L.H., Keyes C.D., 1987, ApJ Suppl.Ser. **65**, 405
Barker T., 1978, ApJ **220**, 193
Barlow M.J., 1987, MNRAS **227**, 161
Barlow M.J., Monk D.J., Walton N.A., Clegg R.E.S., 1992, as quoted by Kingsburgh & Barlow (1992)
Bienaymé O., Robin A.R., Crézé M., 1987, A&A **180**, 94
Cuisinier F., Acker A., Köppen J., 1996, A&A **307**, 215
Faúndez–Abans M., Maciel W.J., 1988, Rev.Mex.A&A **16**, 105
Edvardsson B., Andersen J., Gustafsson B., Lambert D.J., Nissen P.E., Tomkin J., 1993, A&A **275**, 101
Fuchs B., Dettbarn C., Wielen R., 1994, in *Ergodic Concepts in Stellar Dynamics*, eds. V.G.Gurzadyan, D.Pfenniger, Springer, Heidelberg, p.34
Fuchs B., Dettbarn C., Wielen R., 1995, IAU Symp. **169**, in press
Jahreiß H., Wielen R., 1983, IAU Symp. **76**, 277
Kaler J.B., 1970, ApJ **160**, 887
Kaler J.B., 1980, ApJ **239**, 78
Kingsburgh R.L., Barlow M.J., 1992, MNRAS **257**, 317
Kingsburgh R.L., Barlow M.J., 1994, MNRAS **271**, 257
Köppen J., Acker A., Stenholm B., 1991, A&A **248**, 197
Maciel W.J., Köppen J., 1994, A&A **282**, 436
Matteucci F., François P., 1989, MNRAS **239**, 805
Meusinger H., Reimann H.-G., Stecklum B., 1991, A&A **245**, 57
Pagel B.E.J., 1989, in *Evolutionary phenomena in galaxies*, eds. J.E.Beckman, B.E.J.Pagel, Cambridge Univ.Press, Cambridge, p.201
Pagel B.E.J., 1992, IAU Symp. **149**, 133
Peimbert M., 1978, IAU Symp. **76**, 215
Pottasch S.R., 1996, å307561
Rauch T., Köppen J., Werner K., 1994, A&A **286**, 543
Samland M., Köppen J., Acker A., Stenholm B., 1992, A&A **264**, 184
Sommer-Larsen J., Antonuccio-Delogu, 1993, MNRAS **262**, 350
Tylenda R., Acker A., Stenholm B., Köppen J., 1992, A&AS **95**, 337
Wielen R., 1977, A&A **60**, 263
Wielen R., Fuchs B., Dettbarn C., 1996, A&A , in press

This article was processed by the author using Springer-Verlag LaTeX A&A style file *L-AA* version 3.